

# Homonuclear Decoupling of $^1\text{H}$ Dipolar Interactions in Solids by means of Heteronuclear Recoupling

Gregory L. Olsen,<sup>[a]</sup> Adonis Lupulescu,<sup>[a]</sup> Jean-Nicolas Dumez,<sup>[a, b]</sup> Lyndon Emsley,<sup>[b]</sup> and Lucio Frydman\*<sup>[a]</sup>

*Dedicated to Professor Shimon Vega on the Occasion of His 70th Birthday*

**Abstract:** Line narrowing has been traditionally achieved in solid-state  $^1\text{H}$  NMR spectroscopy by applying pulse sequences that combine multiple-pulse operations with magic-angle spinning (MAS), to effectively average out the dipole–dipole homonuclear Hamiltonian. The present study explores a new alternative that departs from the usual concept of directly acting on the strongly coupled spins with radio-frequency pulses; instead, we seek to achieve a net homonuclear dipolar decoupling in solids by exploring the reintroduction of MAS-averaged heteronuclear dipolar couplings between the  $^1\text{H}$  nuclei and directly bonded  $^{13}\text{C}$  or  $^{15}\text{N}$  nuclei.

**Keywords:** dipolar interactions · magic-angle spinning · NMR · organic solids

This recoupling–anti-recoupling (RaR) scheme thus relies on the recoupling of the dipolar interaction with heteronuclear spins, which, under fast MAS, will exceed the strength and will not commute with the homonuclear  $^1\text{H}$ – $^1\text{H}$  coupling one is intending to average out. Subsequent removal (“antiRecoupling”) of these heteronuclear interactions can lead to narrowed  $^1\text{H}$  resonances, without ever pulsing on the aforementioned channel. The line-narrowing properties of RaR are illustrated with numerical simulations and with experiments on model organic solids.

## 1 Introduction

High-resolution  $^1\text{H}$  spectroscopy of arbitrary samples remains one of the “final frontiers” in solid NMR spectroscopy.<sup>[1–3]</sup> As in so many other frontier areas in solid NMR spectroscopy, much of the insight and progress available to us in this field comes from the contributions by the group of Vega.<sup>[4–16]</sup> The challenge of obtaining high-resolution  $^1\text{H}$  solid NMR spectra derives from the fact that protons in rotating solids are coupled by strong multispin, time-dependent and non-commuting homonuclear dipolar interactions, which often lead to broad and featureless spectra. Two general strategies have been exploited to suppress the effects of homonuclear dipolar couplings: magic-angle spinning (MAS)<sup>[17,18]</sup> and decoupling through multiple trains of radiofrequency (RF) pulses.<sup>[19,20]</sup> MAS and multiple-pulse  $^1\text{H}$  decoupling act on the space and spin variables of the homonuclear  $^1\text{H}$ – $^1\text{H}$  dipolar interactions, respectively. The seminal work by the groups of Andrew and Lowe<sup>[17,18]</sup> noted that  $^1\text{H}$  spectral narrowing could be achieved by MAS, even when recognizing the complicating aspects derived from the abovementioned features. Homonuclear dipolar decoupling pulse sequences acting in spin-space were initially developed in static solids, with the aim of averaging out the interaction by continuous<sup>[19]</sup> or discrete<sup>[20]</sup> rotations around an effective averaging axis inclined at the magic angle with respect to the static magnetic field. These original implementations were further refined and combined with MAS in the so-called CRAMPS approach.<sup>[4,14,21–32]</sup> All CRAMPS sequen-

ces use  $^1\text{H}$  RF pulses to manipulate the  $^1\text{H}$ – $^1\text{H}$  interaction directly, and most often optimal results are achieved by a judicious combination of the spin- and spatial-space dipolar averaging procedures. For biomolecular systems, dilution of the proton bath by isotopic labeling provides an efficient third route to high-resolution spectra.<sup>[33–35]</sup> Although highly promising and leading to excellent results, this more recent label-based approach is difficult to generalize to certain systems, such as small organic molecules.

Herein, we explore an alternative approach to homonuclear dipolar decoupling in solids, which does not rely on a direct manipulation of the strongly coupled spins. The proposed pulse sequence, which we dub the recoupling–anti-recoupling (RaR) approach, employs a multiple-pulse sequence, but not one that relies on  $^1\text{H}$  RF pulses to actively average the homonuclear couplings and achieve  $^1\text{H}$  line narrowing. Instead it relies on fast MAS to

[a] G. L. Olsen, A. Lupulescu, J.-N. Dumez, L. Frydman  
Department of Chemical Physics  
Weizmann Institute of Science  
Rehovot 76100 (Israel)  
e-mail: lucio.frydman@weizmann.ac.il

[b] J.-N. Dumez, L. Emsley  
Université de Lyon (CNRS / ENS-Lyon/UCB Lyon 1)  
Centre de RMN à Très Hauts Champs  
5 rue de la Doua  
69100 Villeurbanne (France)

remove a large proportion of the homonuclear dipolar broadening, and then explores the effects of actively reintroducing dipolar interactions with ancillary heteronuclear spins to truncate the MAS-averaged, residual homonuclear  $^1\text{H}$ - $^1\text{H}$  couplings. For the sake of implementing such dominating heteronuclear recoupling, while under the presence of MAS, the REDOR sequence was assayed.<sup>[36,37]</sup> Given the orientation-dependent nature of the REDOR Hamiltonian, however, the coherent dephasing introduced on the free  $^1\text{H}$  evolution by such REDOR application had to be subsequently quantitatively echoed by what we term an anti-recoupling approach, which for simplicity is also a REDOR adaptation. As a consequence, and in contrast to classic CRAMPS decoupling sequences, such RaR line narrowing attempts to truncate away the homonuclear dipolar interactions with minimal pulsing on the  $^1\text{H}$  nuclei. Thus, RaR will not scale at all  $^1\text{H}$  chemical shift interactions. Following a basic theoretical description of the phenomenon, the decoupling performance of a REDOR-based implementation of RaR is analyzed with numerical simulations; experiments on model organic solids are also demonstrated.

## 2 Theoretical Considerations

In a static solid, the Hamiltonian for a system of dipolar-coupled protons and a heteronuclear spin can be written, in the rotating frame, as Equation (1):

$$H = H_0 + H^H + H^{IS} \quad (1)$$

in which  $H_0$  is the chemical-shift interaction,  $H^H$  is the homonuclear  $^1\text{H}$ - $^1\text{H}$  interaction one is attempting to remove, and  $H^{IS}$  is the heteronuclear  $^1\text{H}$ -X interaction. The homonuclear dipolar interaction is given by Equation (2):

$$H^H = \sum_{i>j} \omega_{ij}^{D,H} D_{00}^2(\Omega_{ij}^{PL,H}) \left( 2I_{iz}I_{jz} - \frac{1}{2}(I_{i+}I_{j-} + I_{i-}I_{j+}) \right) \quad (2)$$

in which the sum over all pairs of nuclei,  $\omega_{ij}^{D,H} = -\mu_0\gamma_i^2\hbar/(4\pi r_{ij}^3)$ , is the homonuclear coupling, in which  $r_{ij}$  is the internuclear distance, and  $\Omega_{ij}^{PL,H}$  is the set of Euler angles for the transformation from the principal axis system of the dipolar interaction tensor to the laboratory frame. In high magnetic fields, the large difference in Zeeman frequencies between heteronuclear spins truncates the non-secular “flip-flop” term of the dipolar interaction, which can be written as Equation (3):

$$H^{IS} = \sum_i \omega_{i1}^{D,IS} D_{00}^2(\Omega_{i1}^{PL,IS}) 2S_{1z}I_{iz} \quad (3)$$

in which  $\omega_{ij}^{D,IS} = -\mu_0\gamma_i\gamma_s\hbar/(4\pi r_{ij}^3)$  is the heteronuclear coupling. A key difference between the homo- and heteronuclear dipolar interactions appearing in Equation (1) is that the former entails a sum of non-commuting interactions, whereas the latter, similar to the isotropic/anisotropic chemical shift offset, does not. This distinction is particularly relevant when considering MAS experiments. When the sample is spun at the magic angle at a rate  $\omega_r$ , the orientation-dependent components of the anisotropic shift and dipolar interactions become time dependent. The Hamiltonian can then be written as Equation (4):

$$H(t) = \sum_{m \neq 0} H_{0,m} e^{im\omega_r t} + \sum_{m \neq 0} H_m^H e^{im\omega_r t} + \sum_{m \neq 0} H_m^{IS} e^{im\omega_r t} \quad (4)$$

in which the terms  $H_{0,m}$ ,  $H_m^{IS}$ , and  $H_m^H$  can be calculated by using standard rotational properties of spherical tensors. Main features of the evolution resulting from introducing this time dependence can be understood in the framework of average Hamiltonian theory, which describes the system's approximate state at the conclusion of every rotor period,  $\tau_r = 2\pi/\omega_r$ . Using the decomposition in Equation (4), this average Hamiltonian can be written as Equation (5):

$$\bar{H} = H_{CS} + \sum_{m \neq 0} \frac{1}{m\omega_r} [H_m^H, H_{-m}^H] + \sum_{m \neq 0} \frac{2}{m\omega_r} [H_m^{IS}, H_{-m}^{IS}] + \sum_{m \neq 0} \frac{2}{m\omega_r} [H_{0,m}, H_{-m}^H] + \dots \quad (5)$$

in which  $H_{CS}$  is the sole surviving isotropic interaction and arises from the chemical shifts. Dominant among the commutators that follow this term one is trying to observe unhindered is usually  $[H_m^H, H_{-m}^H]$ , involving a sum of terms of the form  $\kappa_{ijk}\omega_{ij}^D\omega_{ik}^D I_{iz}I_{j+}I_{k-}$ , in which  $\kappa_{ijk}$  is a geometrical factor. Equation (5) highlights the fact that, given the homogeneous nature of the homonuclear dipolar interaction, that is, its non-self-commuting nature at different times, multispin  $^1\text{H}$ - $^1\text{H}$  couplings will not be completely averaged out by MAS. Additional line broadening also comes from the fact that the homo- and heteronuclear interactions, as well as homonuclear couplings and the shift anisotropy, do not commute with each other.

As Equation (5) also illustrates, however, MAS will result in an effective scaling down of these interfering homonuclear coupling terms by means of their  $\omega_r^{-1}$  dependence. Together with this direct effect, an additional line narrowing will arise from the truncation of the MAS-averaged dipolar interaction by the isotropic chemical-shift differences: given the transverse spin components of the former and the purely longitudinal  $I_z$  nature of the latter, these two interactions will not commute. Given sufficiently large chemical shift offset differences, sufficient spectral resolution might become available. Even at

the highest available frequencies, however, these combined mechanisms (MAS and offset-driven truncations) are insufficient to obtain truly high-resolution spectra; hence the usual rationale to actively involve multiple-pulse  $^1\text{H}$ – $^1\text{H}$  dipolar averaging sequences in addition to the MAS. As an alternative to these RF multiple pulses on the  $^1\text{H}$  nuclei, however, one might consider the introduction of the term that further truncates the averaged  $^1\text{H}$ – $^1\text{H}$  dipolar coupling. The RaR mechanism aims to achieve such a truncation by reintroducing a large chemical-shift-difference-like interaction term derived from heteronuclear couplings in directly bonded  $^1\text{H}$ –S pairs, which can reach several tens of kHz. If one considers the use of such a recoupling sequence, the ensuing average Hamiltonian should include one more additional term [Eq. (6)]:

$$\bar{H}_{\text{rec}} = \sum_i \bar{\omega}_{i1} I_{iz} S_{1z} \quad (6)$$

in which the sum is over the  $^1\text{H}$  nuclei directly bonded to the S spin,  $\bar{\omega}_{i1}$  is the average dipolar coupling for the  $^1\text{H}$ –S pairs, and all other heteronuclear couplings are neglected. An evolution under an average Hamiltonian that includes the term in Equation (6) may show a significantly reduced effect of the residual  $^1\text{H}$ – $^1\text{H}$  couplings, in proportion to  $\kappa_{ijk} \omega_{ij}^D \omega_{ik}^D / \bar{\omega}_{i1}$ .

It follows from these considerations that a judicious reintroduction of the heteronuclear dipolar interactions could serve homonuclear decoupling,  $^1\text{H}$  line narrowing, purposes. A variety of pulse sequences have been developed to reintroduce the heteronuclear dipolar interaction,<sup>[36,38–41]</sup> often with the aim of measuring internuclear distances. Herein, we chose the REDOR sequence,<sup>[36]</sup> which relies on rotor-synchronized trains of  $180^\circ$  pulses to reintroduce the heteronuclear couplings being averaged away by MAS. In one of the simplest implementations, REDOR relies on applying two such pulses per rotor period  $\tau_R$ , acting on either one of the nuclear partners involved. The most robust forms of REDOR recoupling have been shown to result if these pulses are alternated among the two nuclear species and suitably supercycled.<sup>[37]</sup> In the present instance, however, we applied them entirely on the  $^1\text{H}$ -bound heteronucleus channel to enable a free and unscaled  $^1\text{H}$  evolution over the course of the experiment.

While applying a conventional REDOR-based recoupling of the heteronuclear dipolar interaction may truncate homonuclear couplings as desired, it will also impart a strong and undesirable anisotropy-based dephasing to the freely evolving  $^1\text{H}$  spins. A key property of the effective heteronuclear dipolar interaction under recoupling, however, is that its sign can be inverted by simple manipulations; in the case of REDOR, all that is needed to effectively reverse the sign of a heteronuclear dipolar evo-

lution is skipping one of the two  $180^\circ$  pulses acting per rotor period. It is thus possible to rewind the phase accumulated under a REDOR recoupling period by applying an anti-recoupling, which is a second REDOR pulse train of identical format and duration, but missing its initial  $180^\circ$  inversion. In RaR decoupling, this sign inversion halfway through the evolution period ensures that there is no net effect of the recoupled interaction on the observed  $^1\text{H}$  evolution. Other recoupling schemes could be used in the evolution period provided that their effect can be refocused, but these were not considered. Attention was solely focused on the pulse sequence shown in Figure 1a. In the final experiments, this block was actually used within a 2D NMR sequence incorporating the abovementioned REDOR-based RaR protocol along its indirect domain, and a subsequent direct domain detection of the heteronucleus affecting the RaR process for the sake of a clearer assessment of line-narrowing achieved by the directly recoupled proton(s).

With these hypotheses at hand, a series of numerical simulations on model spin systems were carried out to confirm or dismiss the predictions of a potential “RaR decoupling effect” appearing on  $^1\text{H}$  line shapes. Instead of simulating full 2D correlation experiments, each peak was simulated independently by considering a system consisting of one carbon and all the protons in a single molecule. Typical results arising from such numerical simulations (see Section 3. Methods for further details) on a small organic molecule, such as L-tyrosine, are shown in Figure 1b and c. The  $^1\text{H}$  evolution signal was obtained in these simulations by “observing” transverse  $^1\text{H}$  magnetization in the corresponding density matrices at the end of the evolution period for the  $^{13}\text{C}$ -bonded proton. As illustrated in Figure 1c, the main conclusion of such approximated simulations is that, at a spinning frequency  $\geq 40$  kHz, a very significant line narrowing of the  $^1\text{H}$  lines is indeed observed when the RaR block is applied. This effect is particularly pronounced for the  $\text{CH}_2$  protons, presumably reflecting the orientation dependence of the different heteronuclear dipolar couplings within the moiety. For most crystallites, this will result in a sizable effective spectral separation that will efficiently truncate the coupling between the two  $^1\text{H}$  nuclei of the  $\text{CH}_2$  group. While the quantitative description of such a strongly coupled spin system is not generally achievable with numerical simulations, these calculations provided a sufficient qualitative motivation to justify further experimental investigations. These are presented in the following sections.

### 3 Methods

The first series of experiments testing the abovementioned considerations was performed with a custom-made tripeptide,  $[\text{U-}^{13}\text{C},^{15}\text{N}]\text{LAF}$  (leucine-alanine-phenylala-

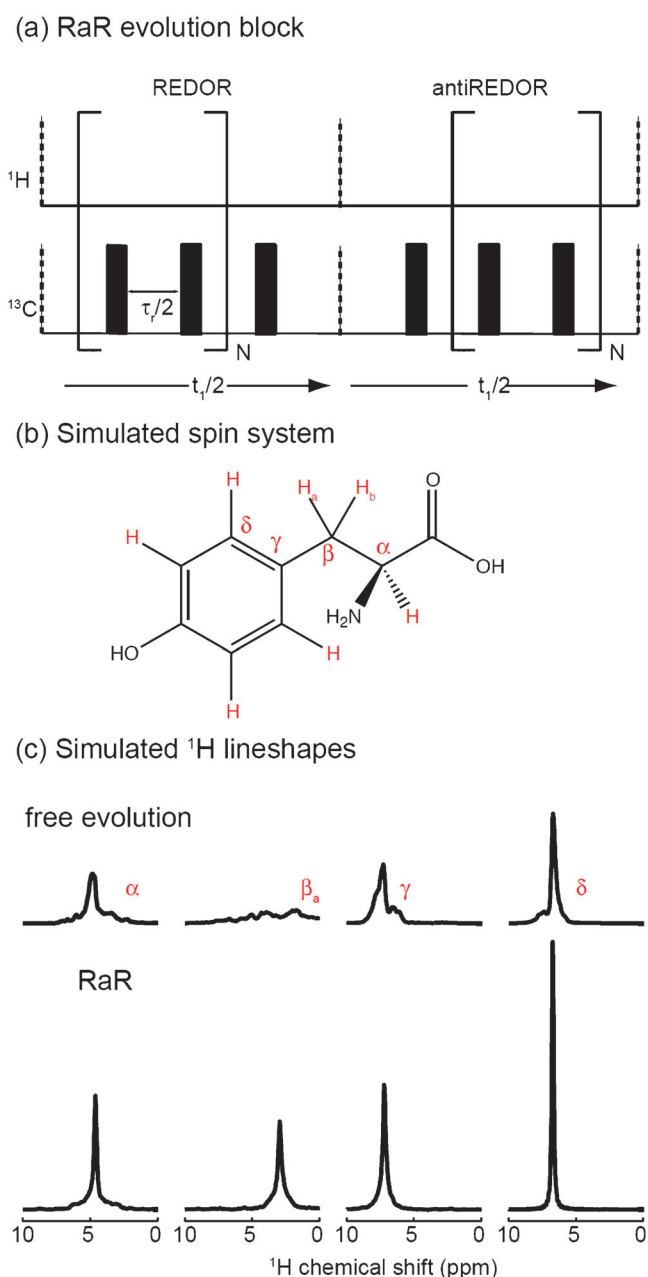


**Figure 1.** (a) REDOR-based RaR pulse sequence for homonuclear  $^1\text{H}$ – $^1\text{H}$  decoupling. (b) Spin system used in numerical simulation of the RaR evolution: each simulation uses the seven carbon-bonded protons of L-tyrosine (shown in red) and a single carbon  $i = \alpha, \beta, \delta,$  or  $\epsilon$ . (c) Comparison between simulated line shapes for RaR evolution and free evolution at a spinning frequency of 40 kHz.

nine), on a Varian VNMRS spectrometer operating at a  $^1\text{H}$  Larmor frequency of 600 MHz. A 1.6 mm triple-resonance Varian probe capable of achieving stable MAS frequencies of up to 40 kHz was used in these acquisitions. 1D  $^1\text{H}$  MAS spectra and 1D  $^{13}\text{C}$  CPMAS data were recorded at a spinning frequency of 39062 Hz. 2D  $^1\text{H}$ – $^{13}\text{C}$  HETCOR spectra<sup>[42, 43]</sup> of the various kinds illustrated in Figure 2a and b were then recorded. These included real-

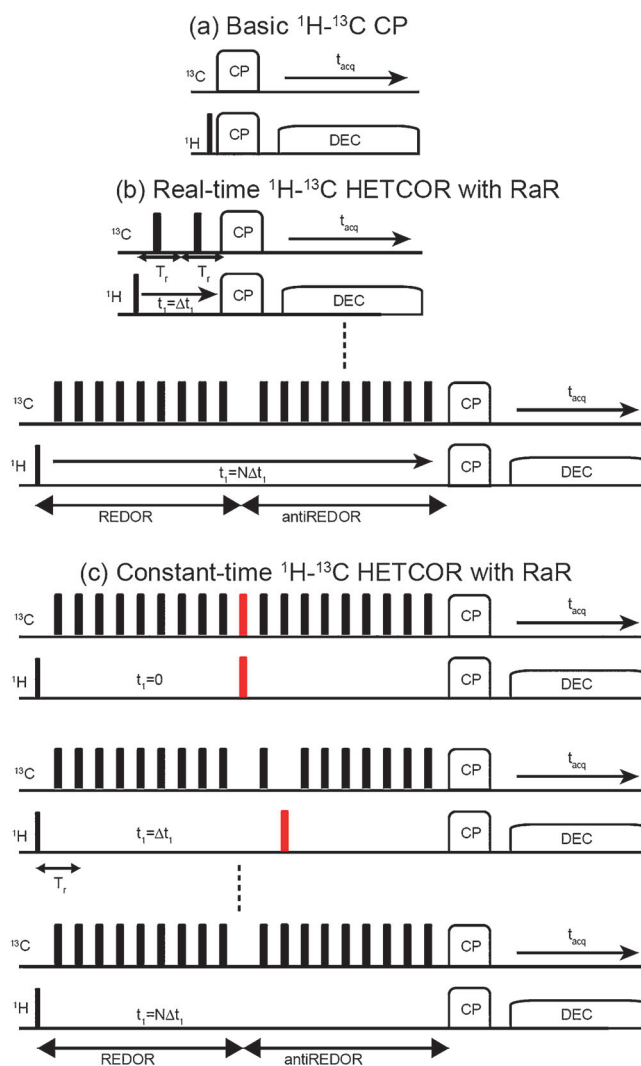


**Figure 2.** Various pulse sequences used and compared in this study. (a) Simple  $^{13}\text{C}$ -detected acquisition. (b) Real-time 2D  $^1\text{H}$ – $^{13}\text{C}$  heteronuclear correlation (HETCOR) experiment employing REDOR-based RaR decoupling during the indirect domain  $^1\text{H}$  evolution period. Only the first and last increments are shown, for a sequence with a maximum evolution time of 10 rotor periods. The RaR  $180^\circ$  trains had fixed phases  $\{xyxy\dots xyx[x]yxy\dots yxyx\}$ , in which  $[x]$  denotes the central (usually missing)  $180^\circ$  pulse. (c) Constant-time version of the same experiment, illustrating the first, second, and last increments of the 2D series. These experiments were run using an  $\{x, x, y, y, -x, -x, -y, -y\}$  phase cycle on the  $^1\text{H}$  'moving  $180^\circ$ ' (red) pulse. All acquisitions used an eight-pulse train of rotor-synchronized inversions with fixed-phases  $\{xyxyxyxy\}$ .

time acquisitions incorporating RaR collected at a spinning frequency of 35714 Hz (rotor period  $\tau_R = 28 \mu\text{s}$ ) with an acquisition time of 12.5 ms; 25 increments of  $2 \tau_R$  in the indirect dimension, resulting in a maximum evolution time of 1.34 ms; a recycle delay of 1 s; and 176 averages, resulting in a total acquisition time of 1.2 h. These experiments were compared against counterparts, the evolution periods of which consisted of a simple free evolution (Fig-

ure 2a). Constant time 2D  $^1\text{H}$ - $^{13}\text{C}$  HETCOR spectra were also recorded, at a spinning frequency of 39062 Hz ( $\tau_{\text{R}} = 25.6 \mu\text{s}$ ) with an acquisition time of 6.6 ms, 22 increments of  $4 \tau_{\text{R}}$  in the indirect dimension, resulting in a maximum evolution time of 2.15 ms; a recycle delay of 1 s; and 288 averages, resulting in a total acquisition time of 1.8 h. Once again, the evolution periods in these constant-time implementations consisted of either a free evolution or a RaR block (Figure 2b). In the RaR blocks, a  $^{13}\text{C}$  nutation frequency of 192 kHz was used for the refocusing pulses. In all of these experiments, the indirect-domain  $^1\text{H}$  evolution period was followed by a short cross-polarization period (contact time of  $60 \mu\text{s}$ ), which enabled a site-specific  $^1\text{H} \rightarrow ^{13}\text{C}$  polarization transfer step; a train of  $\pi$  pulses was used for heteronuclear decoupling<sup>[44,45]</sup> during acquisition because this was a superior alternative at these fast spinning rates.

Further experiments were performed on a commercial sample of  $[\text{U-}^{13}\text{C}]$ L-isoleucine on a Bruker Avance III spectrometer operating at a  $^1\text{H}$  Larmor frequency of 500 MHz. A 1.3 mm probe was used and all spectra were obtained at a MAS frequency of 60 kHz ( $\tau_{\text{R}} = 16.7 \mu\text{s}$ ). Real-time 2D  $^1\text{H}$ - $^{13}\text{C}$  HETCOR spectra were recorded with an acquisition time of 30 ms; 256 increments of  $2 \tau_{\text{R}}$  in the indirect dimension, resulting in a maximum evolution time of 8.5 ms; a recycle delay of 2.5 s; and 8 averages, resulting in a total acquisition time of 1.4 h. The evolution period consisted of either free evolution, of a RaR block (Figure 2a), or of an eDUMBO-PLUS-1<sup>[29]</sup> block used to obtain a comparison against an alternative CRAMPS-type contemporary sequence. In the RaR blocks, a  $^{13}\text{C}$  nutation frequency of 100 kHz was used for the refocusing pulses. For eDUMBO-PLUS-1, a  $^1\text{H}$  nutation frequency of 167 kHz was used. Cross-polarization was used with a short contact time of  $100 \mu\text{s}$  for the polarization transfer step and TPPM<sup>[46]</sup> was used for heteronuclear decoupling during acquisition.

Numerical simulations of the kind described in the preceding section were performed with SPINEVOLUTION.<sup>[47]</sup> In each simulation, the initial density matrix was  $\sigma_0 = \sum I_{j-}$ , in which the sum was over all protons; the observable was the transverse magnetization of the proton bonded to carbon  $i$  at the end of the evolution block. Powder averaging was obtained with a ZCW set of 50 orientations. All experimental and simulated data were processed using Matlab.

## 4 Results

The experimental implementations of the RaR scheme, using the pulse sequence shown in Figure 2a, clearly demonstrate its homonuclear decoupling and  $^1\text{H}$  line narrowing potential. A  $^{13}\text{C}$ -enriched tripeptide, leucine-alanine-phenylalanine (LAF), is selected here to illustrate a variety of experiments carried out on various kinds of proton-

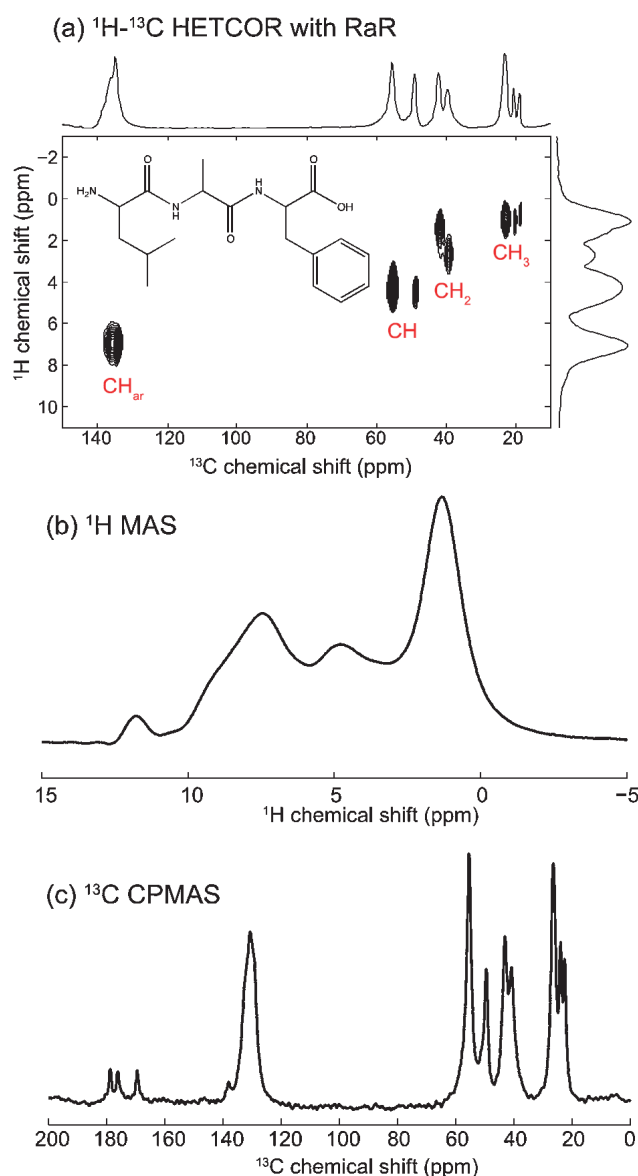


**Figure 3.** (a) 2D  $^1\text{H}$ - $^{13}\text{C}$  HETCOR spectrum obtained for the tripeptide  $[\text{U-}^{13}\text{C}, ^{15}\text{N}]$ LAF using RaR decoupling during evolution. Projections are shown on the sides. The chemical structure of LAF is shown in the inset. The 1D  $^1\text{H}$  MAS (b) and  $^{13}\text{C}$  CPMAS spectra (c) of  $[\text{U-}^{13}\text{C}, ^{15}\text{N}]$ LAF are also shown.

bearing groups. Basic  $^1\text{H}$ - $^{13}\text{C}$  2D HETCOR spectra of LAF, together with reference  $^1\text{H}$  and  $^{13}\text{C}$  1D spectra, are shown in Figure 3. Line shapes extracted from these acquisitions are shown individually in Figure 4, focusing in particular on a comparison between the  $^1\text{H}$  profiles obtained with RaR compared with those obtained with just free MAS evolution. The line-narrowing effect of the RaR sequence is clearly observed from these correlations for all of the sites. Experimental line widths are reported in Table 1, quantifying these observations. Remarkably, as seen in the simulations, the line-narrowing effect of RaR appears to be most significant for the case of  $\text{CH}_2$  groups.

**Table 1.** Experimental  $^1\text{H}$  line widths obtained with real-time and constant-time 2D  $^1\text{H}$ – $^{13}\text{C}$  HETCOR experiments on  $[\text{U-}^{13}\text{C},^{15}\text{N}]\text{LAF}$  with a RaR or free evolution period.

Chemical shift [ppm]	Atom type	Line width [kHz]		Line width [Hz]	
		Real time		Constant time	
		Free	RaR	Free	RaR
130	$\text{CH}_{\text{ar}}$	1.1	0.9	580	400
53	$\text{CH}_{\text{a}}$	1.3	1.1	[a]	[b]
46	$\text{CH}_{\text{b}}$	0.9	0.7	380	330
40	$\text{CH}_{2\text{a}}$	5	0.8	[c]	400
38	$\text{CH}_{2\text{b}}$	5	1	[c]	570
23	$\text{CH}_{3\text{a}}$	1.4	0.7	680	360
21	$\text{CH}_{3\text{b}}$	0.9	0.7	380	330
19	$\text{CH}_{3\text{c}}$	1.2	0.6	420	320

[a] Not resolved. [b] Resolved. [c] Not observed.

Further narrowing of  $^1\text{H}$  resonances can, in general, be obtained in the indirect dimension of 2D experiments when a constant-time implementation is used.<sup>[48]</sup> REDOR-based RaR decoupling can be implemented in a constant-time fashion by choosing a fixed number of rotor periods, and shifting a  $^1\text{H}$  refocusing  $\pi$  pulse by a rotor period for each increment (cf. Figure 2b). A  $^{13}\text{C}$   $\pi$  pulse is then either added or removed to preserve the desired sign of the average heteronuclear dipolar coupling. A clear improvement in resolution can be seen in Figure 4b for the constant-time RaR experiments, with line widths reported in Table 1. This improvement comes at a cost in sensitivity, which is an expected feature of such a constant-time experiment. Again, the  $\text{CH}_2$  protons are the most significantly affected because they become observable with RaR, while they are broadened beyond detection when no decoupling is used.

Finally, Table 2 reports line widths obtained on a sample of  $[\text{U-}^{13}\text{C}]\text{L-isoleucine}$ , the spectra of which are shown in Figure 5. This time the comparison centers on evaluating the performance of the RaR-based decoupling concept, with results arising from one of the most efficient homonuclear dipolar decoupling pulse sequences: eDUMBO-PLUS-1.<sup>[29]</sup> These experiments were performed with spinning at 60 kHz, under conditions for which eDUMBO-PLUS-1 has been optimized.

**Table 2.** Experimental  $^1\text{H}$  line widths obtained with real-time 2D  $^1\text{H}$ – $^{13}\text{C}$  HETCOR experiments on  $[\text{U-}^{13}\text{C}]\text{L-isoleucine}$  with a free, RaR, or a eDUMBO-PLUS-1 evolution period.

Chemical shift [ppm]	Atom type	Line width [Hz]		
		Free	RaR	DUMBO <sup>[a]</sup>
61	CH	780	750	490
37	CH	1300	850	500
26	$\text{CH}_2$	1920	990	890
11–17 <sup>[b]</sup>	$\text{CH}_3$	965	730	380

[a] Corrected to account for the scaling factor. [b] The three signals are comparable and an average is given.

The comparisons in Table 2 reveal that the line widths obtained with the present implementation of RaR are not as good as those of advanced CRAMPS protocols. RaR decoupling, however, benefits from an absence of chemical-shift scaling. Indeed, a significant limitation of numerous strategies that aim at suppressing the homonuclear dipolar interactions with  $^1\text{H}$  RF pulses is a concomitant reduction of the chemical-shift interaction.<sup>[3]</sup> Perfect decoupling scales the chemical shift by a factor of  $1/\sqrt{3}$ , while any increase in the chemical-shift scaling factor comes at a cost in decoupling efficiency of the RF sequence.<sup>[49]</sup> In addition, many sequences yield offset-dependent chemical-shift scaling. While modern CRAMPS sequences provide high, offset-independent scaling factors, changes in the chemical-shift dimension still complicate spectral analysis, especially for unknown compounds. In contrast, the RaR sequence does not involve RF manipulations of the  $^1\text{H}$  spins, and thus, leaves the chemical-shift interaction unchanged (Table 2).

## 5 Discussion

The RaR mechanism relies on a strong heteronuclear dipolar interaction, to truncate the homonuclear dipolar interaction. In organic solids, only directly bonded pairs are expected to have a strong enough dipolar coupling to succeed in this. As a result, when  $^{13}\text{C}$  spins are used as ancillary spins, only  $^{13}\text{C}$ -bonded protons will be efficiently decoupled. The related concept of using  $^1\text{H}$ -bonded ancillary spins to decouple the  $^1\text{H}$ – $^1\text{H}$  interaction can be found in solution-state NMR spectroscopy in sequences that exploit bilinear rotation decoupling (BIRD).<sup>[50–52]</sup> In the case of  $^{13}\text{C}$ -aided decoupling for natural-abundance compounds, RaR is best employed in the evolution period of a  $^{13}\text{C}$ -detected correlation experiment, which ensures that only decoupled protons are observed. The limitation in sensitivity is then intrinsic to the correlation experiments and does not come as an additional cost due to using RaR decoupling. In addition, and in contrast to

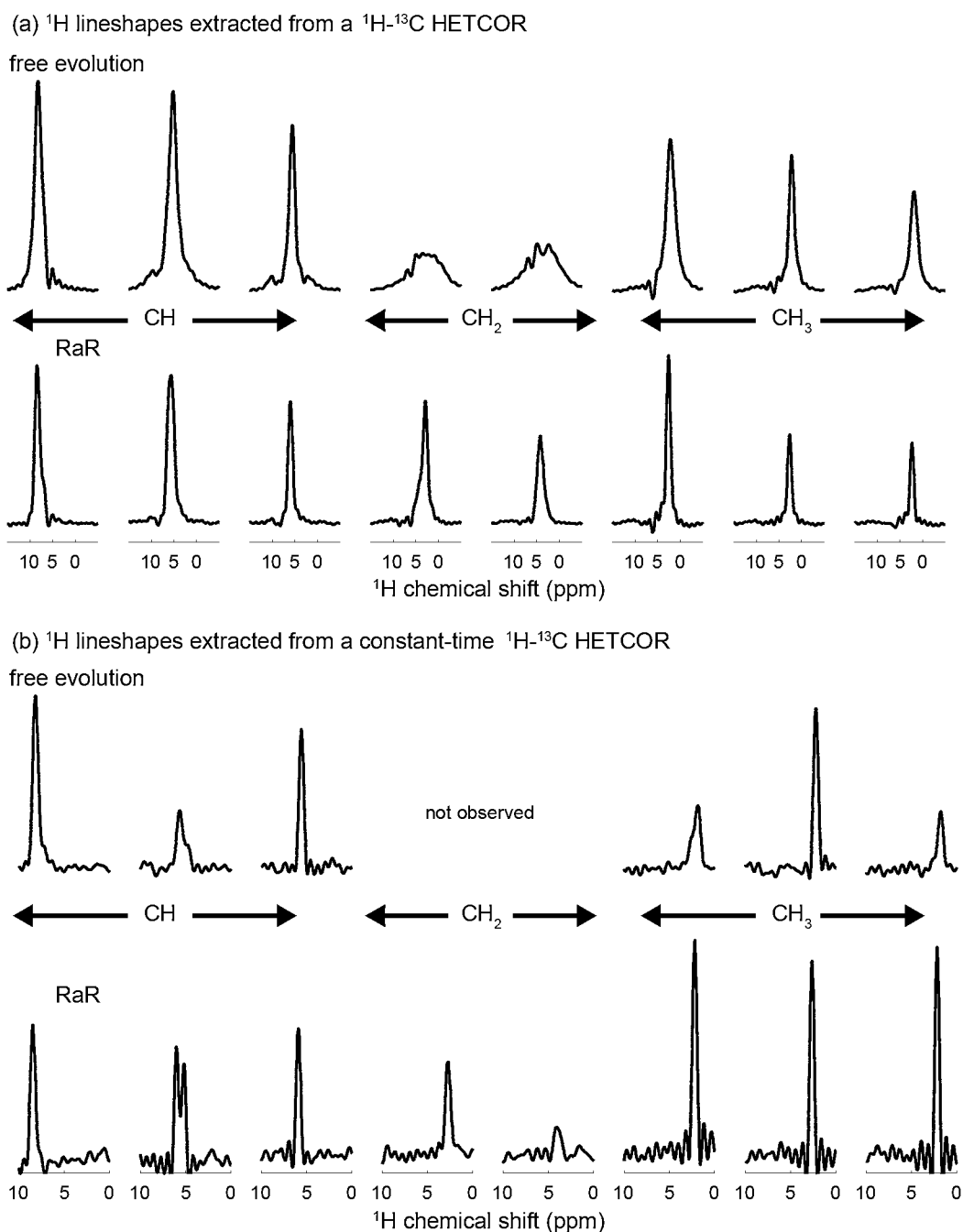


**Figure 4.** Comparison of line shapes obtained in a real-time (a) and a constant-time (b) 2D  $^1\text{H}$ - $^{13}\text{C}$  HETCOR experiments on  $[\text{U-}^{13}\text{C},^{15}\text{N}]\text{LAF}$  with a RaR or free evolution period.

BIRD decoupling, the RaR block is also applicable to a fully  $^{13}\text{C}$ -enriched sample. The results shown in Figure 4 and Table 1 were obtained with a  $^{13}\text{C}$ -enriched sample and comparable line narrowing was observed with natural abundance compounds (data not shown). Although the reasoning behind the RaR sequence is based on a single  $^{13}\text{C}$  spin,  $^{13}\text{C}$ - $^{13}\text{C}$  interactions do not seem to interfere with the decoupling mechanism. In addition, while non- $^{13}\text{C}$ -bonded protons would dominate the signal for direct

$^1\text{H}$  detection in natural-abundance compounds, a windowed implementation of RaR decoupling with  $^1\text{H}$  would be conceivable for such enriched systems.

In summary, we have shown how the effective  $^1\text{H}$ - $^1\text{H}$  dipolar interactions can be reduced in MAS experiments with no direct RF manipulation of the protons. The RaR scheme relies on the heteronuclear dipolar interaction to truncate the homonuclear dipolar interaction. Its line-narrowing properties have been demonstrated in numerical

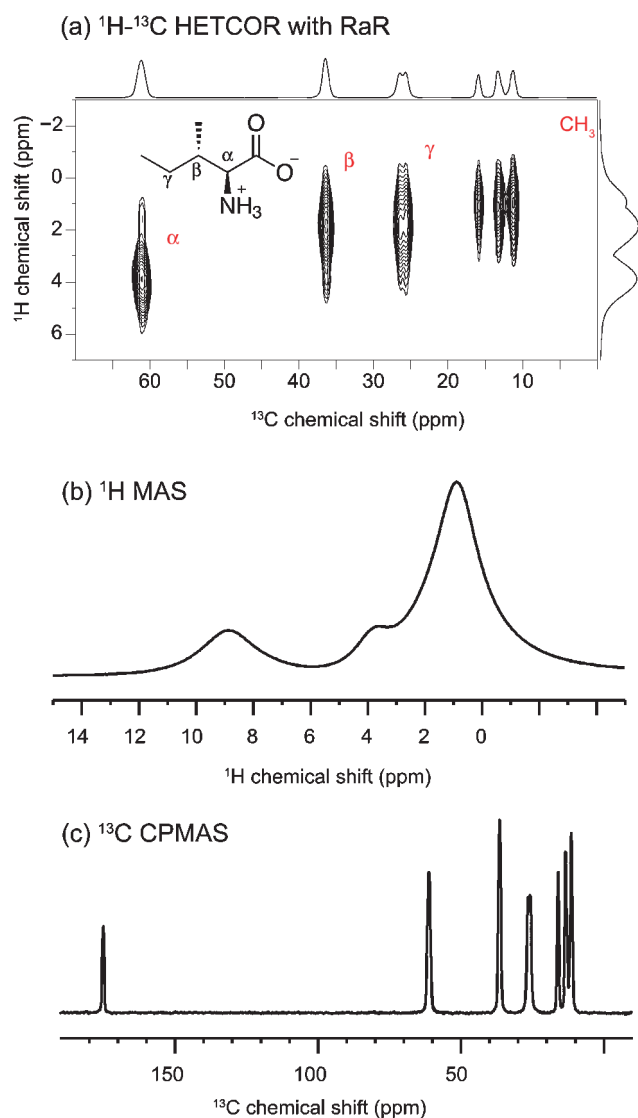


**Figure 5.** (a) 2D  $^1\text{H}$ – $^{13}\text{C}$  HETCOR spectrum obtained for the amino acid  $[\text{U-}^{13}\text{C}]$ L-isoleucine using RaR decoupling during evolution; spectral projections are shown on the sides. The chemical structure of L-isoleucine is shown as an inset. The 1D  $^1\text{H}$  MAS (b) and  $^{13}\text{C}$  CPMAS spectra (c) of  $[\text{U-}^{13}\text{C}]$ L-isoleucine are also shown.

simulation and 2D  $^1\text{H}$ – $^{13}\text{C}$  correlation experiments. RaR decoupling has the significant advantage of leaving the  $^1\text{H}$  chemical-shift interaction unchanged. Because it relies on an entirely new mechanism, it may open the way up for a new class of homonuclear dipolar decoupling sequences.

## Acknowledgments

First and foremost, we would like to acknowledge Prof. S. Vega for the stimulating atmosphere that, in all areas of magnetic resonance, he provides for us dwellers of Perlman's 2nd floor. Financial support from ERC Advanced

Grant (#246754), the Marie Curie Action ITN META-FLUX (project 264780), EU'S BioNMR Grant (#261863), a Helen and Kimmel Award for Innovative Investigation, and the generosity of the Perlman Family Foundation, are gratefully acknowledged.

## References

- [1] A. Lesage, *Phys. Chem. Chem. Phys.* **2009**, *11*, 6876–6891.
- [2] P. K. Madhu, *Solid State Nucl. Magn. Reson.* **2009**, *35*, 2–11.
- [3] P. Hodgkinson, *Annu. Rep. NMR Spectrosc.* **2011**, *72*, 185–223.
- [4] E. Vinogradov, P. K. Madhu, S. Vega, *Chem. Phys. Lett.* **1999**, *314*, 443–450.
- [5] E. Vinogradov, P. K. Madhu, S. Vega, *Chem. Phys. Lett.* **2000**, *329*, 207–214.
- [6] E. Vinogradov, P. K. Madhu, S. Vega, *J. Chem. Phys.* **2001**, *115*, 8983–9000.
- [7] E. Vinogradov, P. K. Madhu, S. Vega, *Chem. Phys. Lett.* **2002**, *354*, 193–202.
- [8] L. Bosman, P. K. Madhu, S. Vega, E. Vinogradov, *J. Magn. Reson.* **2004**, *169*, 39–48.
- [9] E. Vinogradov, P. K. Madhu, S. Vega, *Top. Curr. Chem.* **2005**, *246*, 33–90.
- [10] M. Leskes, P. K. Madhu, S. Vega, *J. Chem. Phys.* **2006**, *125*, 124506.
- [11] M. Leskes, P. K. Madhu, S. Vega, *Chem. Phys. Lett.* **2007**, *447*, 370–374.
- [12] M. Leskes, R. S. Thakur, P. K. Madhu, N. D. Kurur, S. Vega, *J. Chem. Phys.* **2007**, *127*, 024501.
- [13] M. Leskes, P. K. Madhu, S. Vega, *J. Chem. Phys.* **2008**, *128*, 052309.
- [14] M. Leskes, S. Steuernagel, D. Schneider, P. K. Madhu, S. Vega, *Chem. Phys. Lett.* **2008**, *466*, 95–99.
- [15] M. Leskes, P. K. Madhu, S. Vega, *J. Magn. Reson.* **2009**, *199*, 208–213.
- [16] M. Leskes, P. K. Madhu, S. Vega, *Prog. Nucl. Magn. Reson. Spectrosc.* **2010**, *57*, 345–380.
- [17] E. R. Andrew, A. Bradbury, R. G. Eades, *Nature* **1958**, *182*, 1659–1659.
- [18] I. J. Lowe, *Phys. Rev. Lett.* **1959**, *2*, 285–287.
- [19] M. Lee, W. I. Goldburg, *Phys. Rev.* **1965**, *140*, A1261–A1271.
- [20] J. S. Waugh, L. M. Huber, U. Haeberlen, *Phys. Rev. Lett.* **1968**, *20*, 180–182.
- [21] P. Mansfield, *Phys. Lett. A* **1970**, *32*, 485–486.
- [22] W. K. Rhim, D. D. Elleman, R. W. Vaughan, *J. Chem. Phys.* **1973**, *59*, 3740–3749.
- [23] B. C. Gerstein, R. G. Pembleton, R. C. Wilson, L. M. Ryan, *J. Chem. Phys.* **1977**, *66*, 361–362.
- [24] D. P. Burum, W. K. Rhim, *J. Chem. Phys.* **1979**, *71*, 944–956.
- [25] D. P. Burum, M. Linder, R. R. Ernst, *J. Magn. Reson.* **1981**, *44*, 173–188.
- [26] A. Bielecki, A. C. Kolbert, M. H. Levitt, *Chem. Phys. Lett.* **1989**, *155*, 341–346.
- [27] D. E. Demco, S. Hafner, H. W. Spiess, *J. Magn. Reson. Ser. A* **1995**, *116*, 36–45.
- [28] D. Sakellariou, A. Lesage, P. Hodgkinson, L. Emsley, *Chem. Phys. Lett.* **2000**, *319*, 253–260.
- [29] E. Salager, J.-N. Dumez, R. S. Stein, S. Steuernagel, A. Lesage, B. Elena-Herrmann, L. Emsley, *Chem. Phys. Lett.* **2010**, *498*, 214–220.

- [30] Z. Gan, P. K. Madhu, J.-P. Amoureux, J. Trebosc, O. Lafon, *Chem. Phys. Lett.* **2011**, *503*, 167–170.
- [31] M. E. Halse, L. Emsley, *Phys. Chem. Chem. Phys.* **2012**, *14*, 9121–9130.
- [32] P. K. Madhu, X. Zhao, M. H. Levitt, *Chem. Phys. Lett.* **2001**, *346*, 142–148.
- [33] B. Reif, C. P. Jaroniec, C. M. Rienstra, M. Hohwy, R. G. Griffin, *J. Magn. Reson.* **2001**, *151*, 320–327.
- [34] V. Chevelkov, K. Rehbein, A. Diehl, B. Reif, *Angew. Chem. Int. Ed.* **2006**, *45*, 3878–3881.
- [35] M. Hologne, V. Chevelkov, B. Reif, *Prog. Nucl. Magn. Reson. Spectrosc.* **2006**, *48*, 211–232.
- [36] T. Gullion, J. Schaefer, *J. Magn. Reson.* **1989**, *81*, 196–200.
- [37] J. R. Garbow, T. Gullion, *J. Magn. Reson.* **1991**, *95*, 442–445.
- [38] T. G. Oas, R. G. Griffin, M. H. Levitt, *J. Chem. Phys.* **1988**, *89*, 692–695.
- [39] A. Brinkmann, M. H. Levitt, *J. Chem. Phys.* **2001**, *115*, 357–384.
- [40] C. P. Jaroniec, B. A. Tounge, J. Herzfeld, R. G. Griffin, *J. Am. Chem. Soc.* **2001**, *123*, 3507–3519.
- [41] X. Zhao, M. Eden, M. H. Levitt, *Chem. Phys. Lett.* **2001**, *342*, 353–361.
- [42] P. Caravatti, G. Bodenhausen, R. R. Ernst, *Chem. Phys. Lett.* **1982**, *89*, 363–367.
- [43] P. Caravatti, L. Braunschweiler, R. R. Ernst, *Chem. Phys. Lett.* **1983**, *100*, 305–310.
- [44] A. Lupulescu, L. Frydman, *J. Chem. Phys.* **2011**, *135*, 134202.
- [45] X. Filip, C. Tripon, C. Filip, *J. Magn. Reson.* **2005**, *176*, 239–243.
- [46] A. E. Bennett, C. M. Rienstra, M. Auger, K. V. Lakshmi, R. G. Griffin, *J. Chem. Phys.* **1995**, *103*, 6951–6958.
- [47] M. Veshkort, R. G. Griffin, *J. Magn. Reson.* **2006**, *178*, 248–282.
- [48] A. Lesage, L. Duma, D. Sakellariou, L. Emsley, *J. Am. Chem. Soc.* **2001**, *123*, 5747–5752.
- [49] E. Salager, J.-N. Dumez, L. Emsley, M. H. Levitt, *J. Magn. Reson.* **2011**, *212*, 11–16.
- [50] J. R. Garbow, D. P. Weitekamp, A. Pines, *Chem. Phys. Lett.* **1982**, *93*, 504–509.
- [51] J. A. Aguilar, M. Nilsson, G. A. Morris, *Angew. Chem. Int. Ed.* **2011**, *50*, 9716–9717.
- [52] A. Lupulescu, G. L. Olsen, L. Frydman, *J. Magn. Reson.* **2012**, *218*, 141–146.

Received: September 9, 2013

Accepted: November 5, 2013

Published online: February 2, 2014